Journal of Alloys and Compounds 509 (2011) 9598–9603

Contents lists available at ScienceDirect

Journal of Alloys and Compounds

journal homepage: www.elsevier.com/locate/jallcom

Strong correlation between structural, magnetic and transport properties of non-stoichiometric $Sr_2Fe_xMo_{2-x}O_6$ ($0.8 \leq x \leq 1.5$) double perovskites

Y. Markandeya [a], K. Suresh [b], G. Bhikshamaiah [a,*]

[a] Department of Physics, Osmania University, Hyderabad 500007, India
[b] International Advanced Research Centre for Powder Metallurgy and New Materials (ARCI), Hyderabad 500005, India

ARTICLE INFO

Article history:
Received 3 May 2011
Received in revised form 22 June 2011
Accepted 23 June 2011
Available online 18 July 2011

Keywords:
Oxide materials
Sol–gel process
X-ray diffraction
Crystal structure
Magnetic measurements
Magnetoresistance

ABSTRACT

$Sr_2Fe_xMo_{2-x}O_6$ (x = 0.8, 0.9, 1.0, 1.1, 1.2, 1.3, 1.4 and 1.5 wt.%) (SFMO) double perovskite oxides of different compositions have been prepared by sol–gel method. These materials were subjected to X-ray diffraction and found that crystal structure changes from tetragonal to cubic around x = 1.2 wt.%. Lattice parameters and unit cell volume have been calculated using X-ray diffraction data. Magnetization studies have been carried out using Vibrating Sample Magnetometer ranging from −15 kOe to +15 kOe and saturation magnetization (M_s) has been determined. Electrical resistivity and magnetoresistance studies have been carried out in the magnetic field range of −40 kOe to +40 kOe keeping the temperature constant at 5, 150 and 300 K using standard four-probe method. Resistivity studies have also been carried out in the temperature ranging from 5 to 300 K keeping the magnetic field constant at 0, 10, 20 and 40 kOe. Maximum degree of Fe/Mo ordering (η_{max}) of SFMO has been calculated and compared with magnetic and transport properties. It has been found that there is a strong correlation between 3 parameters η_{max}, M_s and MR (%), i.e. all of them show a maximum at x = 1.0 wt.% and decreases as x deviates from 1.0 in SFMO. It has been also found that there is a different resistivity behavior between $x \leq 1.2$ wt.% and $x > 1.2$ wt.% samples of SFMO. Semiconductor metal transition temperature was found to be maximum at x = 1.0 wt.%.

1. Introduction

The double perovskite of the type $A_2BB'O_6$ (A = Sr, Ca, Ba; B = Fe, Cr, Ga, Mg, Mn, etc.; and B′ = Mo, Re, W, etc.) have been extensively studied for the past several years due to the substantial Low Field Magneto Resistance (LFMR) at room temperature [1]. As part of general studies on double perovskites recently, an article on the effect of indium doping on structural, magnetic and transport properties of ordered Sr_2FeMoO_6 double perovskite has been published from this laboratory [2]. Sr_2FeMoO_6 is an ordered double perovskite of the $A_2BB'O_6$ type with Fe and Mo atoms alternates on the B and B′ sites, respectively [3]. Sr_2FeMoO_6 compound crystallizes either in tetragonal structure with space group $I4/mmm$ or in cubic with space group $Fm\bar{3}m$ [3–5]. The special interest in these materials is the issue of the intrinsic conduction mechanism, which brings about metallic values of resistance. A ferrimagnetic half-metallic nature was confirmed in this ordered Sr_2FeMoO_6 with localized up-spin electrons of Fe^{3+} and itinerant down-spin electron of Mo^{5+}[6]. Monte Carlo simulation indicated that the magnetic and electron transport properties of $A_2BB'O_6$ are strongly related to the degree of the B/B′-site ordering and anti-site defects (ASDs) of the compound [7–9]. In view of this, a number of experimental studies have been made by doping with several elements at Mo or Fe site and related to degree of ordering of Fe/Mo site or concentration of ASDs with magnetic and transport properties of Sr_2FeMoO_6 [10–14]. Kobayashi et al. [10] and Sugata et al. [11] have studied $Sr_2Fe(W_{1-x}Mo_x)O_6$ by doping W at Mo site and reported that the ground state changes from an antiferromagnetic insulator to a ferromagnetic metal and the degree of Fe/Mo ordering increases by doping W at Mo site. Yuan et al. [14] have studied $Sr_2(Fe_{1-x}Cu_x)MoO_6$ by doping Cu at Fe site and reported that degree of Fe/Mo ordering increase when Cu is heavily doped at Fe site and induces a transition from semiconductor to metal. G.H. Rao et al. [3,15,16] have studied structural, magnetic and transport properties of $Sr_2Fe_xMo_{2-x}O_6$ ($0.8 \leq x \leq 1.5$) and related these properties to the degree of Fe/Mo ordering. However, magnetoresistance studies of $Sr_2Fe_xMo_{2-x}O_6$ have not yet been made so far in literature. Therefore, the authors have made a compressive study of structural, magnetic and magnetoresistance properties of $Sr_2Fe_xMo_{2-x}O_6$ and related to the degree of Fe/Mo ordering in this paper.

2. Experimental

Polycrystalline samples of $Sr_2Fe_xMo_{2-x}O_6$ (x = 0.8, 0.9, 1.0, 1.1, 1.2, 1.3, 1.4 and 1.5 wt.%) (SFMO) were synthesized by sol–gel method [17–19]. Stoichiometric

* Corresponding author. Tel.: +91 4027682242.
E-mail address: gbhyd08@gmail.com (G. Bhikshamaiah).

0925-8388/$ – see front matter © 2011 Elsevier B.V. All rights reserved.
doi:10.1016/j.jallcom.2011.06.108

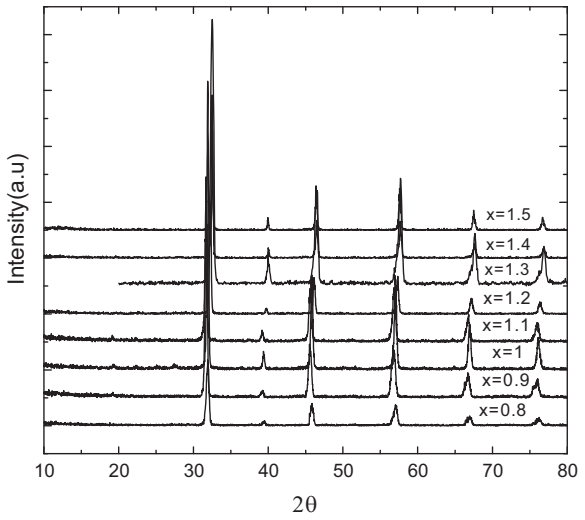

Fig. 1. X-ray diffraction patterns of $Sr_2Fe_xMo_{2-x}O_6$ ($0.8 \le x \le 1.5$ wt.%) samples recorded at room temperature.

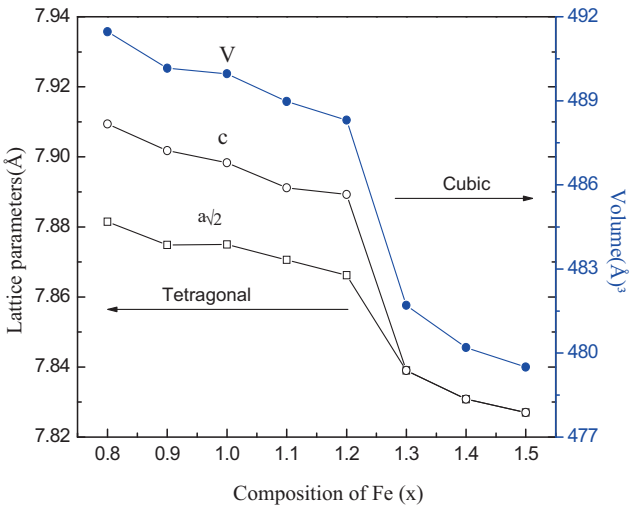

Fig. 2. Variation of lattice parameters (a and c) and unit cell volume (V) with Fe composition in SFMO. The lines are guide to eyes.

amounts of AR grade $Sr(NO_3)_2$, $Fe(NO_3)_2{\cdot}9H_2O$ and H_2MoO_4 were used and powders of SFMO are obtained. These powders are then pressed into pellets of 10 mm diameter and about 2 mm thickness using a die and a hydraulic press by applying a pressure of 1 ton. These pellets were sintered at 1200 °C for 6 h. Subsequently, these pellets were heated at 1000 °C in a stream mixture of 10% H_2/Ar gas for about 3 h for loss of oxygen or reducing the Mo^{6+} to Mo^{5+}. The entire details of preparation of the materials are given in our recent publication [2]. These materials are subjected to X-ray diffraction studies using Philips PW 1830 generator diffractometer with Cu Kα radiation (40 kV × 25 mA) and graphite monochromatic in order to confirm the structure. The magnetization measurements of all samples were measured as a function of magnetic field from −15 kOe to 15 kOe at room temperature using Digital Measurement Systems' Model 880 USA make of Vibrational Sample Magnetometer. Electrical resistivity measurements were carried out at constant magnetic field of 0, 10, 20 and 40 kOe in the temperature range of 5–300 K employing the standard four-probe method using home made resistivity insert along with OXFORD superconducting magnet system. Isothermal magnetoresistance measurements were carried out at 5, 150 and 300 K while varying magnetic field from −40 kOe to 40 kOe. For all the infield measurements magnetic field direction were kept parallel to current direction. The relevant MR (%) has been evaluated using this resistivity data as a function of temperature as well as magnetic filed.

3. Results and discussion

3.1. Crystal structure

X-ray diffraction patterns of various compositions of SFMO are shown in Fig. 1. These patterns reveal that the observed diffraction profiles belong to double perovskite structure of Sr_2FeMoO_6. All the diffraction profiles corresponding to SFMO are shown in Fig. 1. These profiles have been indexed to single phase double perovskite structure. It has been found that $Sr_2Fe_xMo_{2-x}O_6$ crystallizes in tetragonal structure with space group $I4/mmm$ for $0.8 \le x \le 1.2$ wt.% and in cubic structure with space group $Fm\bar{3}m$ for $x > 1.2$ wt.%. The lattice parameters a and c of SFMO ($0.8 \le x \le 1.2$ wt.%) with tetragonal structure have been evaluated using (1 0 1), (1 1 2), (2 0 2), (2 2 0), (3 1 2), (2 2 4) and (1 1 6) X-ray diffraction profiles while lattice parameter a of SFMO ($x > 1.2$ wt.%) with cubic structure have been evaluated using (1 1 1), (0 2 2), (2 2 2), (0 0 4), (2 2 4), (0 4 4) and (0 2 6) X-ray diffraction profiles. The values of lattice parameters a and c, and unit cell volume V of SFMO are given in Table 1. The error in lattice parameters in a and c is found to be ±0.004 Å and ±0.003 Å respectively. Using lattice parameters a and c, unit cell volume (V) has been calculated. The variations of lattice parameter and unit cell volume with composition of Fe in SFMO are shown in Fig. 2. It is found from Fig. 2 that the lattice parameters and unit cell volume decreases with increase of Fe composition in SFMO samples in both tetragonal and cubic phase. Since the ionic radius of Fe^{3+} (0.645 Å) is larger than that of Mo^{5+} (0.61 Å), this decrease might be attributed to cation or oxygen vacancies as observed in many perovskites or valence disproportion [20–22]. Both the vacancy and valence disproportion could lead to the decrease of the lattice parameters and the unit cell volume with the increase of Fe content. It can also be noted from Fig. 2 that the structural transition from tetragonal to cubic lattice structure occurs around $x = 1.2$ wt.% in SFMO.

3.2. Degree of Fe/Mo ordering

In an ordered compound, the degree of Fe/Mo ordering (η) is a characterization of preferential occupation (P) of different atoms on respective sites in a unit cell. For a solid solution $A_{2-x}B_x$ of an ordered phase AB, one can define the degree of ordering η as: $\eta = P_A^{(1)} - P_A^{(2)} = P_B^{(2)} - P_B^{(1)}$, where $P_A^{(1)}$, $P_A^{(2)}$, $P_B^{(1)}$ and $P_B^{(2)}$ are relative occupancies of A and B atoms on A site and B site respectively, i.e. $P_A^{(1)} + P_B^{(1)} = 1$ and $P_A^{(2)} + P_B^{(2)} = 1$. Therefore, when complete disorder occurs, $P_A^{(1)} = P_A^{(2)} = 1 - x/2$, $P_B^{(1)} = P_B^{(2)} = x/2$, and $\eta = 0$. When the maximum ordering is achieved, $P_A^{(1)} = 1$, $P_A^{(2)} = 1 - x$, $P_B^{(1)} = 0$, $P_B^{(2)} = x$, and $\eta_{max} = x$ for A-rich compound ($x < 1$), and $P_B^{(2)} = 1$, $P_B^{(1)} = x - 1$, $P_A^{(2)} = 0$, $P_A^{(1)} = 2 - x$ and $\eta_{max} = 2 - x$ for B-rich compounds ($x > 1$). In the present case the non-stoichiometric $Sr_2Fe_xMo_{2-x}O_6$, Fe and Mo ions alternatively occupy the B and B′ sites respectively in a double perovskite $A_2BB'O_6$ unit cell [3]. The maximum degree of Fe/Mo ordering $\eta_{max} = 2 - x$ for Fe-rich compounds ($x > 1.0$ wt.%) and $\eta_{max} = x$ for Mo-rich compounds ($x < 1.0$ wt.%). Then the value of η_{max} has been calculated. The variation of η_{max} of SFMO as a function of x is shown in Fig. 3(a). It shows that η_{max} is maximum at $x = 1.0$ wt.% and then decreases as x deviates from 1.0 in SFMO materials. It implies that a departure of x from 1.0 in SFMO leads to increase of disorder of the Fe/Mo-site.

3.3. Magnetization measurements

Magnetic field dependence of magnetization of SFMO taken at 300 K is shown in Fig. 4. The values of saturation magnetization (M_S) of all the samples were evaluated from Fig. 4 and given in Table 1. The variation of M_S with composition of Fe is shown in Fig. 3(b). It can be seen from the figure that the M_S is maximum when $x = 1.0$ wt.% and decreases when x deviates from 1.0. This shows that M_S is maximum, when the η_{max} is maximum and both of them decrease as x is different from 1.0. The reduction in the value of M_S can be attributed to mis-site (Fe–Mo) imperfection, oxygen

Table 1
Lattice parameters (a and c), unit cell volume (V) and magnetic parameters of the non-stoichiometric $Sr_2Fe_xMo_{2-x}O_6$ ($0.8 \le x \le 1.5$) double perovskites.

	Composition, x [wt.%]							
	0.8	0.9	1.0	1.1	1.2	1.3	1.4	1.5
Lattice parameter, a (Å)	5.574	5.569	5.567	5.566	5.563	7.839	7.831	7.827
Lattice parameter, c (Å)	7.909	7.902	7.898	7.891	7.889	7.839	7.831	7.827
Unit cell volume, V (Å^3)	491.46	490.14	489.54	488.93	488.28	481.70	480.23	479.50
Saturation magnetization, M_s (emu/g) at $T = 300$ K	10.05	15.65	18.07	16.35	4.08	13.86	6.76	5.57

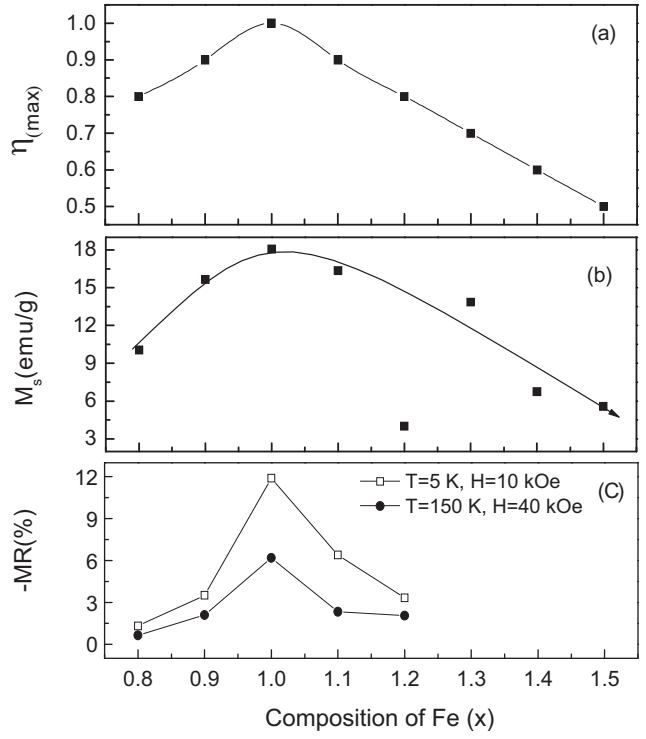

Fig. 3. Variation of (a) maximum degree of Fe/Mo ordering (η_{max}), (b) saturation magnetization (M_s) and (c) MR (%) at $T = 5$ K and $H = 10$ kOe; $T = 150$ K and $H = 40$ kOe with composition of Fe in non-stoichiometric SFMO.

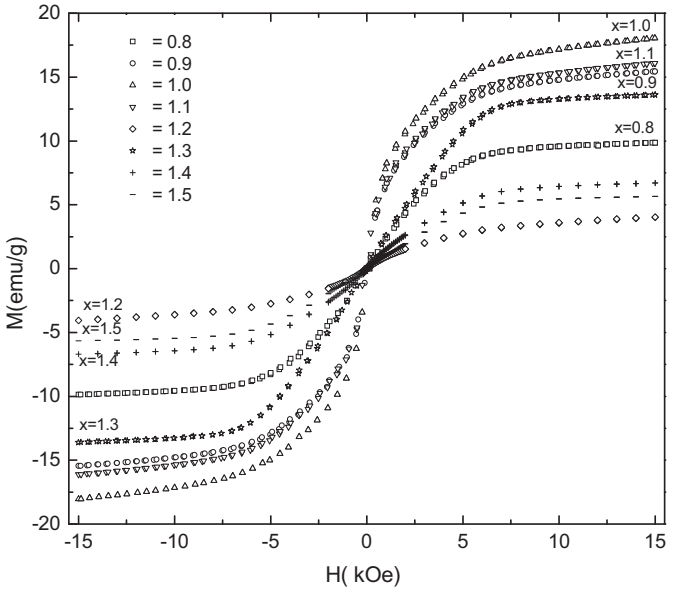

Fig. 4. Magnetic field dependence magnetization (M–H) curves of SFMO of various compositions obtained at room temperature.

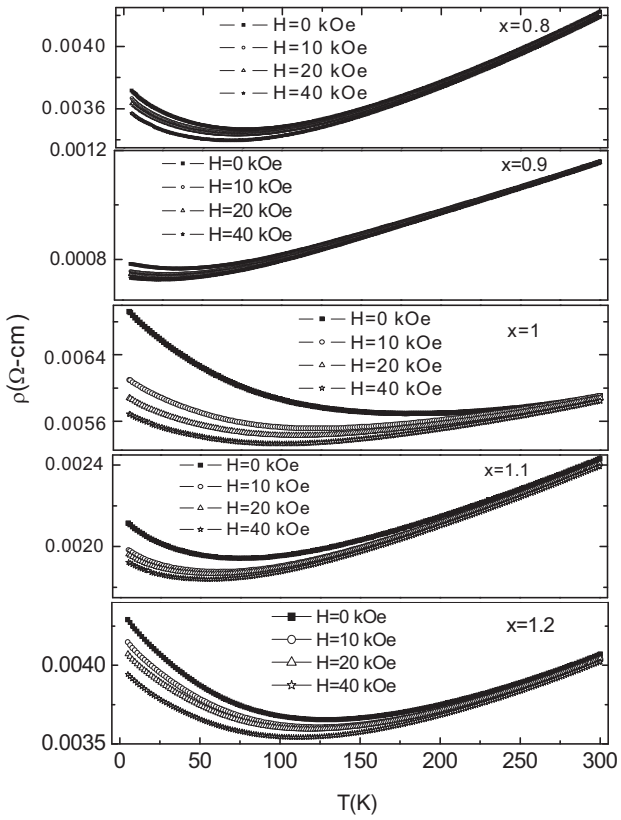

Fig. 5. Variation of resistivity of SFMO ($0.8 \le x \le 1.2$ wt.%) in tetragonal phase as a function of temperature at applied magnetic field of 0, 10, 20 and 40 kOe.

deficiency and valence disproportion [7,9,15]. It is also widely recognized that ASDs diminish M_s because the Fe spins in the Mo site anti-ferromagnetically couple with regular Fe spins. Ogale et al. [7] from Monte Carlo simulation study have reported that the anti-ferromagnetic Fe–O–Fe interaction grows with concentration of ASDs in Sr_2FeMoO_6 and accordingly, the domain Fe contribution to the M_s decreases. However, at $x = 1.2$ wt.%, the large deviation in the value of M_s may be due to the structural transition from tetragonal to cubic lattice. Therefore, the magnetic properties of SFMO compounds depend on the degree of Fe/Mo-ordering.

3.4. Electronic transport properties

3.4.1. Resistivity studies

The variation of electrical resistivity (ρ) of SFMO ($0.8 \le x \le 1.2$ wt.%) in tetragonal phase with temperature in the range from 5 to 300 K keeping magnetic field constant at 0, 10, 20 and 40 kOe is shown in Fig. 5. It has been found from Fig. 5 that the resistivity of Sr_2FeMoO_6 varies between 5.931×10^{-3} and 6.934×10^{-3} Ω-cm at 0 Oe, 5.883×10^{-3} and 6.103×10^{-3} Ω-cm at 10 kOe, 5.894×10^{-3} and 5.881×10^{-3} Ω-cm at 20 kOe and 5.693×10^{-3} and 5.831×10^{-3} Ω-cm at 40 kOe as the temperature is changed from 5 to 300 K. The values of ρ of Sr_2FeMoO_6 obtained

Table 2
Semiconductor–metal transition temperature (T_{SM}) and MR (%) values of the non-stoichiometric $Sr_2Fe_xMo_{2-x}O_6$($0.8 \le x \le 1.2$) double perovskites.

	Composition, x [wt.%]				
	0.8	0.9	1.0	1.1	1.2
T_{SM} (K) at 0 kOe	77.63	34.63	178.92	83.38	132.58
T_{SM} (K) at 10 kOe	73.96	27.48	125.89	59.66	123.63
T_{SM} (K) at 20 kOe	69.81	26.81	112.44	57.90	107.24
T_{SM} (K) at 40 kOe	60.18	22.26	100.54	56.75	105.64
MR (%) at T = 5 K, H = 10 kOe	−1.31	−3.51	−11.90	−6.39	−3.33
MR (%) at T = 5 K, H = 20 kOe	−2.03	−5.03	−15.05	−7.23	−5.12
MR (%) at T = 5 K, H = 40 kOe	−3.72	−6.63	−17.86	−9.04	−8.10
MR (%) at T = 150 K, H = 40 kOe	−0.65	−2.10	−6.18	−2.32	−2.06
MR (%) at T = 300 K, H = 40 kOe	−0.23	−0.75	−1.36	−1.01	−0.76

in the present study are smaller than those reported [1]. This may be due to the difference in preparation method and sintering conditions. From Fig. 5, it is noticed that the resistivity is higher in case of material with maximum degree of Fe/Mo ordering, i.e. x = 1.0 wt.% in SFMO compared to the other compositions in tetragonal phase. The samples with $x \le 1.2$ wt.% have a low resistivity and exhibit a transition from the semiconductor to metal as temperature increases as shown in Fig. 5. The values of semiconductor–metal transition temperature (T_{SM}) have been obtained from this figure and are given in Table 2. From Table 2, it can be seen that T_{SM} decreases with increase of magnetic field. This may be due to the increase of magnetic ordering or alignment of magnetic dipoles with magnetic field. It is observed that for x = 1.0 wt.%, T_{SM} is high as the η_{max} is high at this Fe composition.

The variation of ρ of SFMO for $x > 1.2$ (x = 1.3 and 1.5 wt.%) in cubic phase with temperature in the range of 5–300 K at zero magnetic field is shown in Fig. 6. The electrical resistivity of SFMO for x = 1.3 and 1.5 wt.% exhibit only a semiconductor behavior throughout the temperature range of 5–300 K. The resistivity of these materials is found to be in the range of 1.7×10^0–6×10^2 Ω-cm. The value of ρ is several orders of magnitude more compared to the compounds with $x \le 1.2$ wt.%, which is of the order ranging from 0.75×10^{-3} to 6.8×10^{-3} Ω-cm. This is possibly because of phase transition around x = 1.2 wt.% [3,16]. These result are in agreement with the result of the X-ray diffraction analysis which indicates a structural phase transition from the tetragonal to cubic lattice

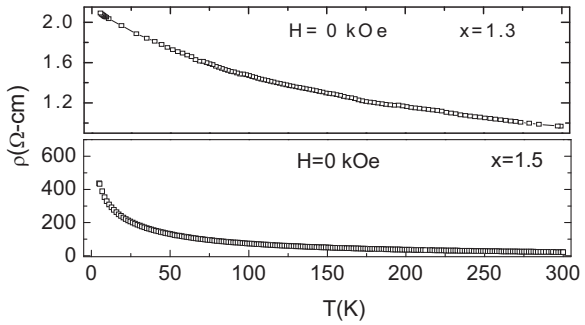

Fig. 6. Variation of resistivity of SFMO (x = 1.3 and 1.5 wt.%) in cubic phase as a function of temperature under zero magnetic field.

around x = 1.2 wt.% [16]. The ρ versus T plots clearly reveal different behavior for $x \le 1.2$ wt.% and $x > 1.2$ wt.%. In order to understand the origin of the semiconducting behavior of samples with $x > 1.2$ wt.%, a detailed analysis of ρ versus T was performed. It was found that a simple activation like dependence of ρ on T cannot account for resistivity data of SFMO (x = 1.3 and 1.5 wt.%) in the temperature range of 5–300 K. This is often the case for insulating oxide samples, as the low-temperature transport trends to be dominated by very low density of localized states introduced by impurities and non-stoichiometry with in the band gap region of the stoichiometric compound, and the ρ appears to be best described by the variable

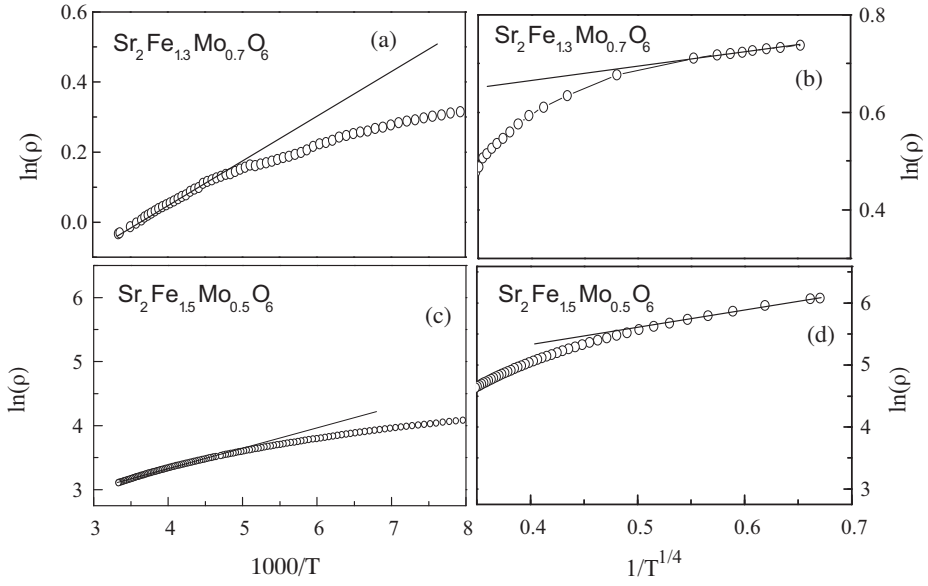

Fig. 7. The dependence of resistivity (ρ) on the temperature (T) in ln(ρ) (ln(Ω-cm)) (a) against 1000/T (1/K) plot for high temperature regime, (b) against $1/T^{1/4}$ ($1/K^{1/4}$) plot for low temperature regime of $Sr_2Fe_{1.3}$ $Mo_{0.7}O_6$ sample, (c) against 1000/T (1/K) plot for high temperature regime and (d) against $1/T^{1/4}$ ($1/K^{1/4}$) plot for low temperature regime of $Sr_2Fe_{1.5}$ $Mo_{0.5}O_6$ sample.

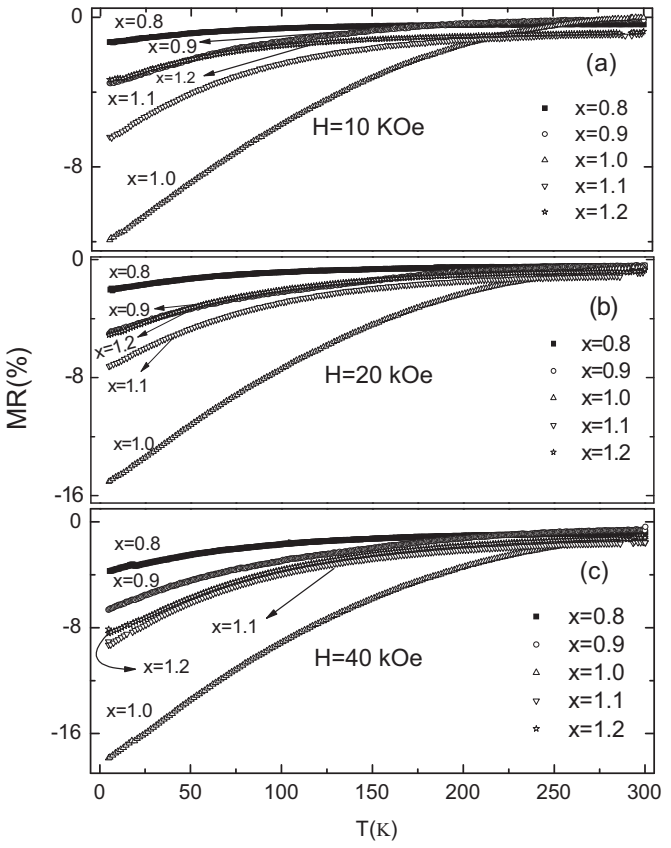

Fig. 8. Variation of MR (%) of SFMO ($0.8 \leq x \leq 1.2$ wt.%) materials with temperature in an applied field of (a) 10 kOe, (b) 20 kOe and (c) 40 kOe.

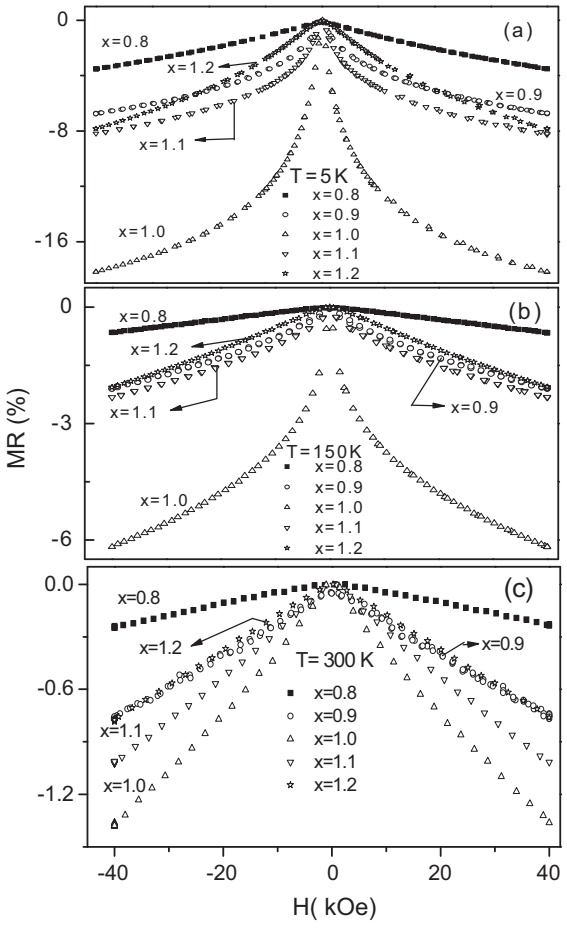

Fig. 9. Variation of MR (%) of SFMO ($0.8 \leq x \leq 1.2$ wt.%) materials with magnetic field at temperatures (a) 5 K, (b) 150 K and (c) 300 K.

range hopping (VRH) mechanism, which is the linear dependence of $\ln(\rho)$ on $1/T^{1/4}$, while the high-temperature behavior is contributed by the thermally activated hopping of the charge carriers across the bad gap, which is the linear dependence of $\ln(\rho)$ on $1/T$ [23]. Fig. 7(a)–(d) shows the dependence of resistivity on the temperature in a $\ln(\rho)$ against $1/T$ plot for high-temperature regime and against $1/T^{1/4}$ plot for low temperature regime for $x = 1.3$ and 1.5 wt.% respectively. In agreement with above analysis, the low-temperature resistivity can be attributed to VRH process while the high-temperature resistivity to a thermally activated hopping of the charge carriers.

3.4.2. Temperature dependent magnetoresistance

The temperature dependence of percentage of magnetoresistance (MR %) at a field 10, 20 and 40 kOe for the samples SFMO ($0.8 \leq x \leq 1.2$ wt.%) are shown in Fig. 8(a)–(c) respectively. MR(%) is defined as $MR(\%) = [\{\rho(H,T) - \rho(0,T)\}/\rho(0,T)] \times 100$, where H denotes the applied field and $\rho(0,T)$ and $\rho(H,T)$ are the resistivity at zero field and H fields respectively at temperature T. The variation of magnitude of MR (%) of all materials is found to increase with decrease of temperature suggesting that the grain boundary effect dominates the MR as temperature decreases [24]. The values of MR (%) at 5 K and different fields at $H = 10$, 20 and 40 kOe are obtained from Fig. 8 and given in Table 2. The variation of MR (%) with composition at 5 K and 10 kOe is shown in Fig. 3(c). It may be noted that the magnitude of MR (%) at 5 K and 10 kOe is maximum at $x = 1.0$ wt.% and then decreases as x deviates from 1.0. It is due that a departure of x from 1.0 in SFMO system tends to increase the ASDs or disorder of the Fe/Mo-site ordering in SFMO compounds there by MR (%) decreases [8,24,25]. Similar trends of MR (%) with composition of Fe were also observed at magnetic field 20 and 40 kOe.

3.4.3. Magnetic field dependent magnetoresistance

The MR (%) of SFMO ($0.8 \leq x \leq 1.2$) were evaluated in the magnetic field range of −40 to 40 kOe at 5, 150 and 300 K. The variation of MR (%) with magnetic field is shown in Fig. 9(a)–(c) at 5, 150 and 300 K respectively for the materials $x \leq 1.2$ wt.%. It can be seen from Fig. 9 that the variation of magnitude of MR (%) increases with increasing magnetic field. There are two mechanisms which contribute to the MR (%) of SFMO double perovskite in the presence of magnetic field. One of them is due to the lowering of spin scattering at grain boundaries upon the application of magnetic field. This mechanism is most effective at low fields and temperatures well below T_C, where the polarization of carriers is large. The other mechanism is an intrinsic one which results from the quenching of spin scattering of the carriers by localized spins. This mechanism dominates the high-field MR [8,25]. The values of MR (%) at 40 kOe and different temperatures at $T = 5$, 150 and 300 K are obtained from Fig. 9 and given in Table 2. The variation of magnitude of MR (%) with x at 40 kOe and 150 K is shown in Fig. 3(c). It can be seen from Fig. 3(c) that the MR (%) at 40 kOe and 150 K is maximum at $x = 1.0$ wt.% and then decreases as composition deviates from 1.0. It is due that a departure of x from 1.0 in the SFMO system tends to increase the ASDs or decrease of Fe/Mo-site ordering in SFMO samples there by MR (%) decreases [8,24,25]. Therefore, it is found from Fig. 9(b) that the magnitude of MR (%) at a given temperature 150 K increases with increase of magnetic field however the magnitude of MR (%) decreases when x deviate from 1.0. Similar trends have been observed at 5 and 300 K as shown in Fig. 9(a) and (c) respectively. The reduction in MR (%) can be attributed to increase of ASDs that reduces the spin polarization of charge carriers [8,25].

4. Conclusions

It has been found that the values of η_{max}, M_s and MR (%) are maximum and decreases as x deviates from 1.0 in SFMO materials, i.e. there exists a strong correlation between structural, magnetic and transport properties in these materials. It is also found that there is a structural transition from tetragonal to cubic around $x = 1.2$ wt.%. Different resistivity behavior has been found for $x \leq 1.2$ wt.% and $x > 1.2$ wt.% materials of SFMO.

Acknowledgments

One of the authors (GB) wish to thank UGC-SERO, Hyderabad for providing financial assistance to carryout this work under the minor research project (File No. MRP-350/04 and Link No. 1350). The authors thank Dr. Rajeev Rawat, Dr. Alok Banerjee of UGC-DAE, Consortium for Scientific Research, Indore for providing magnetoresistance and magnetization facilities. The authors also thank Dr. V. Raghavendra Reddy of UGC-DAE, Consortium for Scientific Research, Indore for his help. The authors express their gratitude to the Head, Department of Physics, Osmania University and the Head, Department of Physics and Principal, Nizam College, Osmania University, Hyderabad for their encouragement.

References

[1] K.I. Kobayashi, T. Kimura, H. Sawada, K. Terakura, Y. Tokura, Nature (Lond.) 395 (1998) 677.
[2] Y. Markandeya, D. Saritha, M. Vithal, A.K. Singh, G. Bhikshamaih, J. Alloys Compd. 509 (2011) 5195.
[3] G.Y. Liu, G.H. Rao, X.M. Feng, H.F. Yang, Z.W. Ouyang, W.F. Liu, J.K. Liang, J. Alloys Compd. 353 (2003) 42.
[4] M. Itoh, I. Ohta, Y. Inaguma, Mater. Sci. Eng. B 41 (1996) 55.
[5] B. Garcia-Landa, C. Ritter, M.R. Ibarra, J. Blasco, P.A. Algarabel, R. Mahendiran, J. Garcĭa, Solid State Commun. 110 (1999) 435.
[6] Y. Tomioka, T. Okuda, Y. Okimoto, R. kumari, K.-I. Kobayashi, Y. Tokura, Phys. Rev. B 61 (2000) 422.
[7] A.S. Ogale, S.B. Ogale, R. Ramesh, T. Venkatesan, Appl. Phys. Lett. 75 (1999) 537.
[8] M. Garcia-Hernandez, J.L. Martinez, M.J. Martinez-Lope, M.T. Casais, J.A. Alonso, Phys. Rev. Lett. 86 (2001) 2443.
[9] L. Balcells, J. Navarro, M. Bibes, A. Roig, B. Martĭinez, J. Fontcuberta, Appl. Phys. Lett. 78 (2001) 781.
[10] K.-I. Kobayashi, T. Okuda, Y. Tomioka, T. Kimura, Y. Tokura, J. Magn. Magn. Mater. 218 (2000) 17.
[11] S. Ray, A. Kumar, S. Majumdar, E.V. Sampathkumaran, D.D. Sarma, J. Phys.: Condens. Matter 13 (2001) 607.
[12] Y. Moritomo, H. Kusuya, T. Akimoto, A. Machida, Jpn. J. Appl. Phys. 39 (2000) L360.
[13] F. Sriti, A. Maignan, C. Martin, B. Raveau, Chem. Mater. 13 (2001) 1746.
[14] C.L. Yuan, Y. Zhu, P.P. Ong, J. Appl. Phys. 91 (2002) 4421.
[15] G.Y. Liu, G.H. Rao, X.M. Feng, H.F. Yang, Z.W. Ouyang, W.F. Liu, J.K. Liang, J. Phys.: Condens. Matter 15 (2003) 2053.
[16] G.Y. Liu, G.H. Rao, X.M. Feng, H.F. Yang, Z.W. Ouyang, W.F. Liu, J.K. Liang, J. Phys. B 334 (2003) 229.
[17] J. Mahai, C. Vazquez, J. Mirza, A. Lopez-Quentela, J. Rivas, T.E. Jones, S.B. Oseroff, J. Appl. Phys. 75 (1994) 6757.
[18] W.H. Song, J.M. Dai, S.L. Ye, K.Y. Wang, J.J. Du, Y.P. Sun, J. Appl. Phys. 89 (2001) 7678.
[19] C.L. Yuan, Y. Zhu, P.P. Ong, Appl. J. Phys. Lett. 82 (2003) 934.
[20] J. Topfer, J.B. Goodenough, Chem. Mater. 9 (1997) 1467.
[21] J.A.M. van Roosmalen, P. van Vlaanderen, E.H.P. Cordfunke, W.L. Ijdo, D.J.W. Ijdo, J. Solid State Chem. 114 (1995) 516.
[22] Y. Takeda, K. Kanno, T. Takada, O. Yamamoto, M. Takano, N. Nakayama, Y. Bando, J. Solid State Chem. 63 (1986) 237.
[23] K. Maiti, N.Y. Vasanthacharya, D.D. Sarma, J. Phys.: Condens. Matter 9 (1997) 7507.
[24] Falak Sher, A. Venimadhav, M.G. Blamire, B. Dabrowski, S. Kolesnik, J. Paul Attfield, Solid State Sci. 7 (2005) 912.
[25] G.D. Anurag Gaur, H.K. Varma, Singh, J. Alloys Compd. 460 (2008) 581.